CHEMBIOCHEM

DOI: 10.1002/cbic.200700706

A Sequential Assignment Procedure for Proteins that have Intermediate Line Widths in MAS NMR Spectra: Amyloid Fibrils of Human CA150.WW2

Johanna Becker,[a] Neil Ferguson,[b] Jeremy Flinders,[a, c] Barth-Jan van Rossum,[a] Alan R. Fersht,[b] and Hartmut Oschkinat*[a]

The second WW domain (WW2) of CA150, a human transcriptional activator, forms amyloid fibrils in vitro under physiological conditions. Based on experimental constraints from MAS NMR spectroscopy experiments, alanine scanning and electron microscopy, a structural model of CA150.WW2 amyloid fibrils was calculated earlier. Here, the assignment strategy is presented and suggested as a general approach for proteins that show intermediate line width. The $^{13}C,^{13}C$ correlation experiments were recorded on fully or partially ^{13}C-labelled fibrils. The earlier ^{13}C assignment (26 residues) was extended to 34 of the 40 residues by direct ^{13}C-excitation experiments by using a deuterated sample that showed strongly improved line width. A 3D HNCTEDOR (transferred-echo double-resonance) experiment with deuterated CA150.WW2 fibrils yielded 14 amide nitrogen and proton resonance assignments. The obtained chemical shifts were compared with the chemical shifts determined with the natively folded WW domain. TALOS (Torsion angle likelihood obtained from shift and sequence similarity) predictions confirmed that, under physiological conditions, the fibrillar form of CA150.WW2 adopts a significantly different β structure than the native WW-domain fold.

Introduction

A number of largely unrelated peptides and proteins oligomerise and aggregate in vitro and in vivo to form a range of insoluble fibrillar structures.[1] A subset of these proteins, including α synuclein and the Aβ peptides, which are involved in Parkinson's and Alzheimer's disease, respectively,[2,3] forms what has become known as amyloid fibrils. Amyloid fibrils appear to be a common manifestation associated with, but not necessarily causal in, the progression of a range of serious diseases collectively known as amyloidoses (e.g., haemodialysis-related amyloidoses or immunoglobulin light-chain deposition) or spongiform transmissible encephalopathies (e.g., nvCJD, BSE).[1] Currently, there is great interest in the mechanisms by which these fibrils form, whether fibrils or oligomeric precursors are toxic and in the structures of relevant conformational states.[4] A better understanding of the origins of these "aggregation" diseases could, perhaps, lead the way for designing more effective therapeutic strategies.

Whilst the exact role of amyloid fibrils in disease states appropriately remains a matter of conjecture,[4,5] they are nonetheless choice subjects of enquiry since they constitute an apparent endpoint in terms of molecular aggregation. Until very recently, however, it was necessary to use low-resolution techniques to characterise amyloid fibrils since their large size (typically >MDa) prevented the use of solution NMR spectroscopy, and the problems in generating single crystals made it extremely difficult to obtain high-resolution information by using standard diffraction techniques. By using low-resolution techniques, it has become clear, however, that unrelated amyloidogenic peptides display common structural properties: they have a diagnostic cross β diffraction pattern with a characteristic 4.7 Å reflection, which is consistent with a structure that contains repeated β strands arranged perpendicular to the long axis of the fibril;[6] when examined by electron microscopy, fibrils are usually unbranched and can be many microns in length;[7] the periodicity of the β structure in fibrils causes them to interact with the histological dyes Congo Red and Thioflavin T,[8,9] which gives rise to diagnostic spectroscopic properties after sample staining.

Recent advances in crystallographic techniques have, however, yielded higher-resolution information about the underlying structures of amyloid fibrils. The crystal structures of short peptides (QNNQQNY and NNQQNY) derived from the yeast prion protein, Sup35, were recently determined by using microcrystals and extremely narrow synchrotron beams. Fibrils formed from these short peptides contain parallel in-register intermolecular β sheets.[10] Each β sheet interacts closely with a second sheet that is antiparallel to the first one, such that the side chains of each sheet interdigitate, and the β sheets are translated by half a strand along the long axis of the fibril with

[a] J. Becker, Dr. J. Flinders, Dr. B.-J. van Rossum, Prof. H. Oschkinat
Structural Biology, Leipniz-Institut für Molekulare Pharmakologie
Robert-Rössle-Strasse 10, 13125 Berlin (Germany)
Fax: (+49) 30-94793-161
E-mail: oschkinat@fmp-berlin.de

[b] Dr. N. Ferguson, Prof. A. R. Fersht
Centre for Protein Engineering, Medical Research Council
Hills Road, Cambridge CB2 2QH (UK)

[c] Dr. J. Flinders
Present address: Department of Pharmaceutical Chemistry
University of California, Genentech Hall, 600 16th Street
San Francisco, CA 94107 (USA)

respect to each other. This interaction is termed a steric zipper and is proposed to form the structural core of amyloid fibrils.[10] Recently, similar arrangements were found in a number of different short peptides derived from several amyloidogenic proteins.[11]

Magic-angle spinning (MAS) NMR is emerging as the tool of choice for characterising structures of amyloid fibrils when these prove refractory to crystallisation (i.e., the majority of known amyloidogenic peptides or full-length proteins). Large β-sheet regions were found for fibrils formed by Aβ(1–40),[12] Aβ(1–42),[13] the K3 peptide from β_2 microglobulin,[14] HET-s-(218–289),[15,16] TTR,[17] α synuclein[18,19] and the islet amyloid polypeptide,[20] by using MAS NMR spectroscopy chemical-shift analysis or hydrogen–deuterium exchange in combination with solution state NMR spectroscopy. MAS NMR spectroscopy studies of Aβ(1–40) also revealed side-chain interactions of residues in different β sheets and these were used to build a structural model.[12,21] However, a different register was found for Aβ(1–42) by mixing of several variants.[13] The monomeric subunits of fibrils formed by the 22 residue K3 peptide of β_2 microglobulin have two β-sheet regions connected by a loop. A number of side-chain contacts between the β sheets was observed; this enabled the calculation of a structure.[14] For HET-s(218–289) four β-strand regions were determined, and found to form two β hairpins.[15]

A wide range of line widths is observed in MAS NMR spectra of different amyloid fibrils depending on their structural homogeneity and their dynamic properties. Fibrils formed by the prion protein HET-s(218–289) or α synuclein yield spectra in which signals from parts of the molecule show favourable, narrow line widths that simplified ^{13}C and ^{15}N resonance assignments.[16,18] In contrast, fibrils formed by Aβ(1–40) showed very broad lines, which made it necessary to employ selective labelling strategies in order to achieve assignments.[12] Relatively broad lines were also observed in spectra of the 22 residue K3 peptide of β_2 microglobulin.[14]

The number of amyloid systems for which structural information on a molecular level could be obtained so far is thus small. To develop a general picture of amyloid structures it is, therefore, desirable to study more amyloid fibrils and to find a way to extract information from MAS NMR spectra that show broad signals. Here, we demonstrate an approach that allows the assignment of MAS NMR spectra of samples that yield intermediate line widths. The resonance assignment can directly be used to determine the β-strand regions in amyloid fibrils from torsion angle likelihood obtained from shift and sequence similarity (TALOS) predictions. Often, this might already be of great value since this kind of analysis can be used to determine experimentally the residues responsible for aggregation. Further, the assignment is a prerequisite for the detection of long-range distance constraints that define the tertiary structure.

The second WW domain of the human transcriptional activator CA150, CA150.WW2, is identical to the murine FBP28 WW domain,[22] which, in its native fold, forms a three-stranded antiparallel β sheet in microseconds.[22,23] However, CA150.WW2 can also form amyloid fibrils under physiological conditions.[24] In an earlier study we presented a structural model of these fibrils based on alanine scanning, electron microscopy and MAS NMR spectroscopy long-range distance constraints. In this study a construct comprising the 37 residue WW domain and three residues from an N-terminal extension was used. Cα and Cβ resonance assignments of 24 of the 40 residues were obtained.[25] The MAS NMR spectra of these fibrils showed intermediate line widths that hindered the use of standard assignment strategies that employ backbone walks based on NCA/NCACX and NCO/NCOCX spectra of ^{15}N- and uniformly or partially ^{13}C-labelled samples.[16,26–29] To circumvent this problem, a novel assignment strategy was used that relied instead on the mixing-time dependence of intra- and inter-residue cross-peaks in ^{13}C spectra of differently labelled samples: a uniformly ^{13}C,^{15}N-labelled sample (u-CA150.WW2), and preparations made from $^{15}NH_4Cl$ and 2-^{13}C-glycerol (2-CA150.WW2) or 1,3-^{13}C-glycerol (1,3-CA150.WW2) as the sole nitrogen and carbon sources, respectively. Furthermore, spectra recorded on a ^{2}H,^{13}C,^{15}N-labelled sample (d-CA150.WW2) displayed improved line widths. Here, this novel assignment strategy is outlined together with

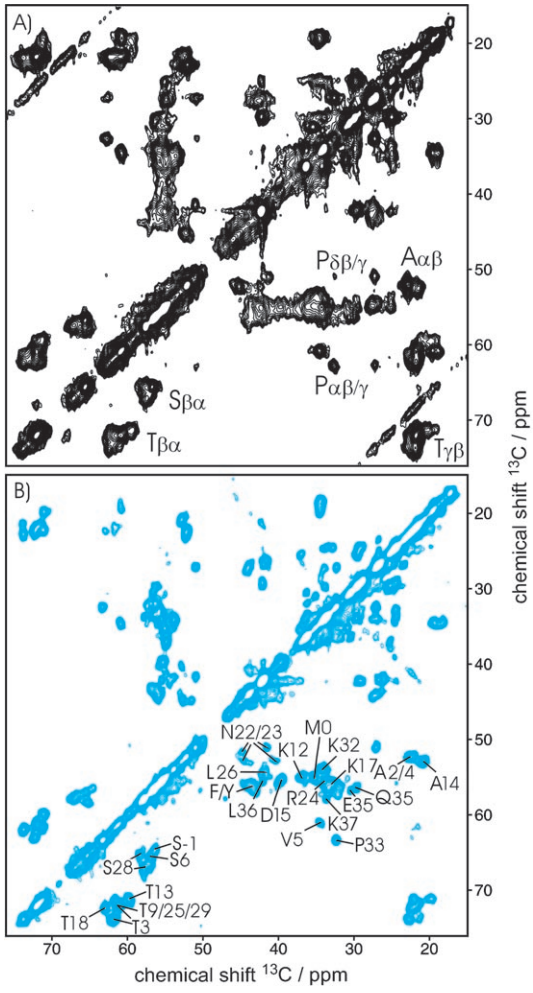

Figure 1. Aliphatic region of ^{13}C–^{13}C correlations. The signal sets of serine, threonine, proline and alanine residues are indicated: A) u-CA150.WW2, 20 ms PDSD, 900 MHz, 10.5 kHz MAS, B) d-CA150.WW2, 1.2 ms RFDR, 900 MHz, 20 kHz MAS, Cα–Cβ correlations are annotated.

the results from direct ^{13}C excitation experiments on d-CA150.WW2, which enabled the identification of residues from the N- and C-terminal regions. This sample was further used in a 3D HNC-transferred-echo double-resonance (TEDOR) experiment, which confirmed the ^{13}C assignment and yielded ^{1}H and ^{15}N assignments. The determined chemical shifts were analysed by using TALOS to obtain secondary structure information, and were compared to the chemical shifts of the natively folded WW domain, which were determined on the same construct by solution NMR spectroscopy.

Results and Discussion

MAS NMR spectra recorded with the fibrils formed by CA150.WW2 are highly reproducible with respect to different preparations and do not change over time (up to two years). CP-PDSD (cross-polarization proton-driven spin-diffusion) spectra of u-CA150.WW2 showed barely resolved cross-peak patterns, for example, for threonine, serine, proline and alanine residues (Figure 1 A). PDSD spectra recorded under the same experimental conditions (10.5 kHz MAS, 900 MHz, 20 ms mixing) with d-CA150.WW2 fibrils, which were formed in 100% H_2O (labile sites were thus protonated), showed better resolved cross-peak patterns. Improved line widths were observed in all spectra recorded with this sample; this was probably due to the reduction of the dipolar couplings concomitant with deuteration, together with possible variations in the dynamic behaviour of the protein. This is in contrast to observations with nanocrystalline ubiquitin,[30] which yields well resolved and efficiently proton decoupled ^{13}C spectra that do not improve upon deuteration.

To our surprise Cα–Cβ cross-peaks were observed in the PDSD spectrum at short mixing times. They occur because the PDSD transfer is most efficient in the vicinity of back-exchanged protons—the amide protons and side chain OH, NH and NH_2. For most amino acids the complete cross-peak pattern was observed by using 100 ms PDSD mixing. Figure 1 B shows a spectrum of d-CA150.WW2, which was recorded by using direct carbon excitation, 20 kHz MAS spinning and 1.2 ms RFDR (radio frequency driven recoupling). At this short mixing time cross-peaks occur mainly between carbon atoms separated by one bond.

To start the assignment procedure, spin systems were assigned to specific residue types based on the labelling pattern expected for samples prepared by using ^{13}C-labelled glycerol as carbon sources.[31] This also helped to simplify the sequential assignment since seven residues occur only once in the sequence of CA150.WW2 Y19F. The well resolved spectra from the deuterated sample were subsequently used to validate and complete the set of spin systems.

A problem occurred concerning the identification of the tyrosine and asparagine spin systems. In several spectra we observed signs of multiple signals for the tyrosines. A sample containing u-^{13}C,^{15}N glycine and alanine, and 2,3-^{13}C,^{15}N phenylalanine and tyrosine, showed more than seven maxima in a Cα–Cβ cross-peak conglomerate in which only signals from the phenylalanine and three tyrosines are expected. In all spectra, multiple Cα–Cβ signals occurred for N22 and N23, and peak doubling was observed for T3 and S28.

To establish sequential assignments, PDSD spectra with longer mixing times were recorded. The spectra on protonated samples that employed 100 ms mixing times allowed Cα–Cα cross-peaks to be observed (Figures 2 A, C and D). At this mixing time, no sequential correlations were observed in CP-PDSD spectra from the deuterated sample. At a mixing time of

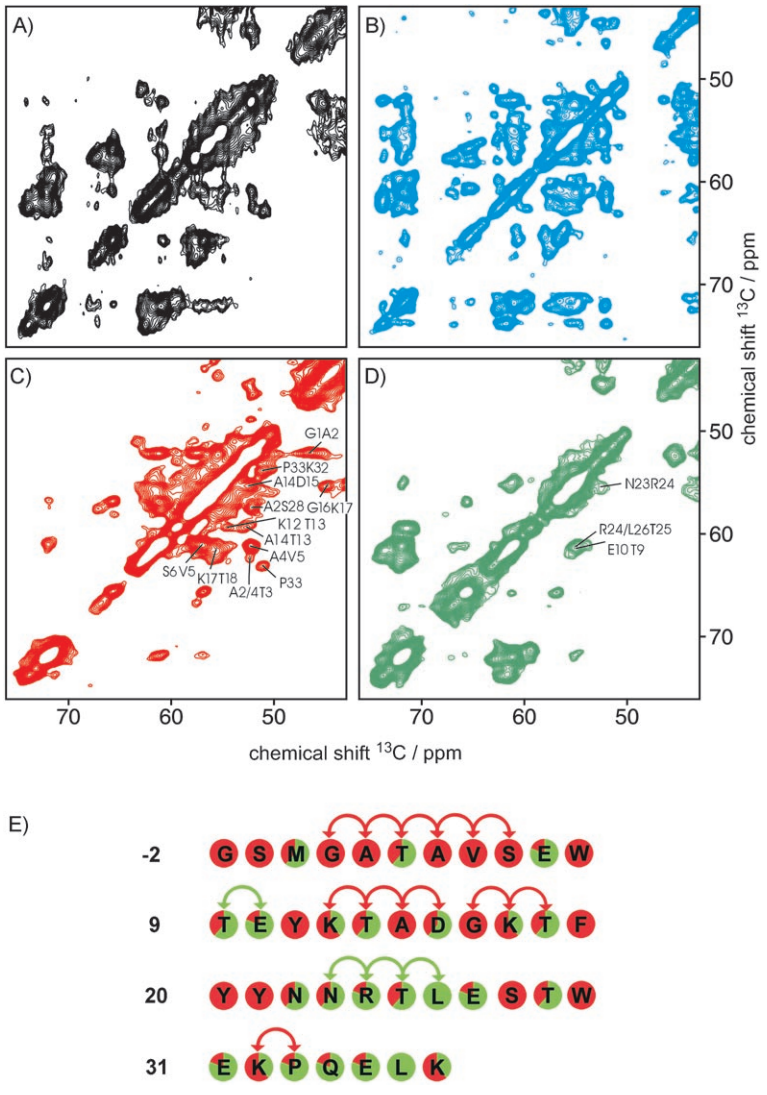

Figure 2. The Cα–Cα region of the differently labelled samples. Cα–Cα correlations are annotated in the spectra of the glycerol labelled samples: A) u-CA150.WW2, 100 ms PDSD, 900 MHz; B) d-CA150.WW2, 400 ms DARR, 900 MHz; C) 2-CA150.WW2, 100 ms PDSD, 700 MHz; D) 1,3-CA150.WW2, 100 ms PDSD, 700 MHz; E) labelling pattern of the glycerol-labelled samples: red and green correspond to the degree of labelling in 2-CA150.WW2 and 1,3-CA150.WW2, respectively, arrows indicate correlations that can be observed in panels C) and D).

400 ms, despite the low abundance of ^{1}H in this sample, many sequential contacts were nonetheless observed (Figure 2B).

In contrast to the uniformly labelled samples, spectra of 2-CA150.WW2 and 1,3-CA150.WW2 only showed Cα–Cα contacts when neighbouring Cα atoms were labelled. This systematic dilution of spins provides better resolved spectra and improved Cα–Cα transfer, hence many Cα–Cα cross-peaks were observed by using 100 ms PDSD mixing time (Figure 2C–E). Strong cross-peaks between neighbouring residues are expected when they have a pure (e.g., alanine, serine) or nearly pure (lysine or glutamic acid) labelling pattern at the Cα site. Accordingly, the spectra of 2-CA150.WW2 and 1,3-CA150.WW2 were expected to contain eight and nine strong Cα–Cα cross-peaks, respectively (Figure 2E).

Several sequential correlations were evident in the spectra of 2-CA150.WW2 (Figure 2C). The cross-peaks G1A2, A4V5, V5S6 and G16K17 were easily identified, as the chemical-shift differences of the corresponding Cα signals were quite large. In addition, some pairs with one or two residues partially labelled in the Cα position gave rise to cross-peaks: (A2/A4)T3, K12T13, T13A14, A14D15 and K17T18. For the proline residue, a cross-peak between K32α and P33δ was observed. An additional cross-peak at 52.2 and 57.6 ppm in the direct and indirect dimensions, respectively, was observed that could not be assigned to a sequential contact and was therefore assumed to be a long-range contact (A2–S28). The expected correlations Y11K12, F19Y20, Y20Y21 were not observed, primarily as a consequence of spectral overlap of Cα resonances and the heterogeneous appearance of the tyrosine residues. The first two residues (G−2,S−1) did not give rise to signals in the spectra of the protonated samples.

Evaluation of the Cα–Cα region in the spectra of 1,3-CA150.WW2 allowed mainly hypotheses for resonance assignments (Figure 2D). In combination with other signals the observed Cα–Cα correlations yielded the assignments T9E10, N23R24, R24T25, T25L26. The Cα chemical shifts of T9, T25 and E10, R24, L26 were very similar and caused spectral overlap. The cross-peaks N22N23 and L26E27 were expected to be very close to the diagonal. No Cα–Cα correlations were observed for P33Q34, Q34E35, E35L36 because these C-terminal residues of the protein apparently exhibited increased mobility compared to the remainder of the sequence (see below).

Further sequential correlations between amino acids were identified by employing longer mixing times (100–400 ms). Cβ–Cβ, Cα–Cγ and Cβ–Cγ cross-peaks were only interpreted as sequential when they occurred in conjunction with sequential cross-peaks of the type discussed above.

A benefit of the deuteration is a better resolution of the cross-peak pattern. In addition, serine and threonine residues showed an efficient PDSD transfer due to the side chain OH, which led to a large number of important correlations at longer mixing times.

Spectra of the deuterated sample recorded with direct ^{13}C excitation showed a group of residues with narrow and intense lines, which were difficult to observe in CP-MAS spectra. The identity of these residues (Q, E, L, K) were consistent with their being part of the C terminus (Q34E35L36K37). This hypothesis was further supported by the up-field shift of the K37-CO resonance, the free COO^{-}. An increased mobility of this part of the protein could explain the appearance of the signals in direct excitation spectra as well as the absence of the expected inter-residue cross-peaks in CP-PDSD spectra.

The combined analysis of all samples led to the assignment of 35 of 40 Cα and 30 of 37 Cβ resonances. Further, several CO (25 of 40) and many side-chain resonances could be assigned (Table 1). Chemical shifts taken from the spectra of the deuterated samples (Table 1, footnote [a]) were corrected for the isotope effect: Cα(Gly) 0.4 ppm, Cα (all other amino acids) 0.3 ppm, Cβ (CD_2 group) 0.5 ppm.[32] After this correction, only few chemical shifts from the deuterated sample deviated by more than 0.5 ppm from the corresponding value of the protonated samples (Table 1, italicised values).

To confirm the assignment and to determine amide nitrogen and proton chemical shifts, a 3D HNC-TEDOR experiment was recorded. This experiment was tailored for our purposes based on the pulse sequences of Michal and Jelinski[33] and Jaroniec et al.[34] (see the Experimental Section). Fourteen amide nitrogen and proton resonance assignments were made based on the known CO and Cα chemical shifts (Table 1). Figure 3 shows slices of the spectrum of the carbonyl and Cα carbon regions at a proton frequency of 9.3 ppm with annotated cross-peak assignments.

The program TALOS was used to predict residue-specific torsion angles and therefore secondary structure. In a first TALOS run the chemical shifts from Table 1 were used, excluding T3 and S28, which showed peak doubling. The results were deemed acceptable when at least two of the five resonances used by TALOS (HA, N, C, CA and CB) were assigned for the corresponding residue, and ≥ 9 out of 10 TALOS predictions were in good agreement. For most residues, the predicted dihedral angles matched the β-sheet region of the Ramachandran plot (Figure 4A, filled symbols). In a second TALOS run further predictions (Figure 4A, open symbols) were obtained by taking triplets into account for which the central residue had only one assigned site (W8, W30, E31) or for which the chemical shifts were deduced in other ways. Specifically, the chemical shifts of the Y/F Cα–Cβ peak conglomerate (Figure 1B) ranged from 55 to 57.5 ppm and 42 to 45 ppm, respectively; this indicates a β-strand conformation for all tyrosines when compared to the TALOS random-coil values of 58.1 and 38.8 ppm for the Cα and the Cβ tyrosine resonances, respectively. Since the tyrosine Cα–Cβ cross-peaks are close together and well within the β-strand chemical shift region (Figure 1B), the values that correspond to the centre of the cross-peak area (56.3 and 43.9 ppm) were used for TALOS analysis. On the basis of the assigned Cα resonance of N23 the two strongest asparagine Cα–Cβ cross-peaks at 51.1–41.5 ppm and 52.3–45.2 ppm in the 1,3-CA150.WW2 20 ms PDSD spectrum were assigned to N22 and N23, respectively.

Residues in the N-terminal tag, the C terminus and residues A14–G16 yielded inconsistent predictions. Therefore, we conclude that two long β strands are present that range from A4 to T13 and from K17 to K32. These are connected by a loop region, which corresponds well to the somewhat broader lines

Table 1. Resonance assignment of CA150.WW2 Y19F in its fibrillar form.

Residue	H	N	C	Cα	Cβ	Cγ	Cδ	Cε/Cζ
G−2			169.9[a]	43.6[a]				
S−1			173.6[a]	55.9[a]	64.5[a]			
M0			174.5[a]	54.9	35.4	31.1		17.2
G1	7.92	108.6	171.3	46.3				
A2	8.66	124.5	177.0	52.1	22.8			
T3	9.40	117.6	*172.7*	*62.3*	73.7	21.8		
					72.2	20.5[a]		
A4	9.90	131.0	*175.9*	52.1	22.7			
V5	9.54	126.7	175.2	60.9	34.5	19.7/18.8		
S6	9.28	123.8	173.2	56.8	65.6			
E7				56.1				
W8					30.4[a]			
T9			173.2	61.0	71.9	22.1		
E10				55.1	*34.5*	36.5	183.8	
Y11								
K12			175.0[a]	54.6	37.0	25.5	29.7	42.2
T13	9.24	113.4	*173.5*	59.3	71.3	*20.0*		
A14	8.00	125.8	*175.9*	52.5	*21.6*			
D15				55.2	39.8	*180.9*		
G16	8.15	108.6	174.6	44.9				
K17	7.92	125.1	176.5[a]	55.2	*33.9*	25.1	*29.7*	42.1
T18	9.01	122.2	171.9	62.3	72.2	21.8		
F19	9.64	129.9	172.2[a]	56.2[a]	43.1[a]	138.6[a]		
Y20								
Y21								
N22								
N23				52.3				
R24				54.9	*34.5*	27.3	43.7	159.6
T25			173.2	60.9	71.8	21.8		
L26				*55.1*	42.2	*27.5*	22.6/21.7	
E27			174.0[a]	55.0	*34.3*	*36.6*	183.6	
S28	8.84	115.9	173.5	57.5	67.0			
			173.9[a]	57.0	65.5			
T29			173.2	61.1	71.9	*21.7*		
W30					30.4[a]			
E31				56.2				
K32	9.21	130.3		53.7	34.5	*25.0*	*29.8*	42.2
P33			176.6	62.9	32.6	27.3	50.9	
Q34			175.9[a]	56.1	29.9	34.0	180.4	
E35			176.1[a]	56.4	30.6	36.3	183.8	
3L6				55.2[a]	42.2	26.9	25.1/23.6	
K37			181.1	57.6	33.9	24.3		

Chemical shifts were determined to an accuracy of ±0.2 ppm, values with lower certainty are underlined. [a] Chemical shifts that were determined with the deuterated sample only; for italic values the corresponding chemical shifts determined on the deuterated sample deviate by more than 0.5 ppm from the given value. The sequence numbering used corresponds to the scheme used in the work of Macias et al.[35]

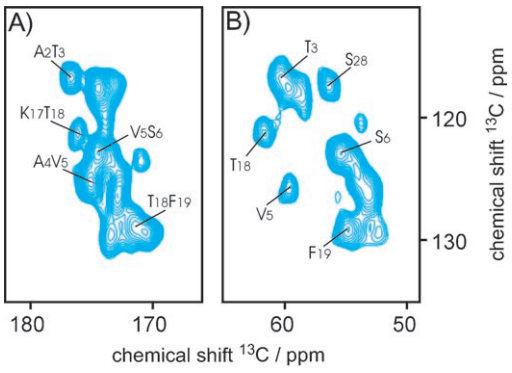

Figure 3. The 2D slices of the HNC-TEDOR experiment at a proton frequency of 9.3 ppm, showing: A) the carbonyl, and B) the Cα region; assigned cross-peaks are annotated.

observed for these residues (A14–G16) in CP-MAS spectra. The occurrence of multiple signals observed for residues Y11, Y20, Y21, N22 and N23 can be explained by different orientations of the aromatic side chains of the tyrosine residues.

The obtained predictions were compared to the TALOS results on the natively-folded, monomeric u-CA150.WW2. Figure 4B shows the three β strands of the WW fold: W8–K12, K17–N22, S28–K32. This corresponds well to the structure determined by Macias et al.[35]

The chemical-shift analysis confirmed that the structural arrangement in native and fibrillar forms of CA150.WW2 is different despite the fact that both have high β-sheet content. The largest difference in the predictions was found for the N terminus and residues R24–E27. These regions are unstructured or are loop regions in the native WW-domain fold, but are part of a β strand in the amyloid fold. The repeating unit of the fibrillar form contains two long β strands (β1 and β2 are 10 and 16 residues long, respectively). By contrast, the native fold has three β strands that are much shorter. Both structures, however, have similarly unstructured regions: residues A14–G16, which correspond to the flexible first loop region of native WW domains,[36] and the C-terminal residues (Q34–K37).

Conclusions

By employing a novel strategy, the usage of a few differently labelled samples enabled the ^{13}C-resonance assignment of CA150.WW2 in its fibrillar form. In addition, a 3D HNC-TEDOR experiment led to the assignment of 35% of the amide nitrogen and proton resonances. Based on this strategy, a partial ^{13}C assignment of CA150.WW2 allowed the identification of long-range correlations in an earlier study, which were used in combination with mutagenesis data and electron microscopy to build a structural model of CA150.WW2 fibrils.[25] The presented ^{13}C-assignment strategy is based on double resonance MAS NMR spectroscopy experiments of high sensitivity and

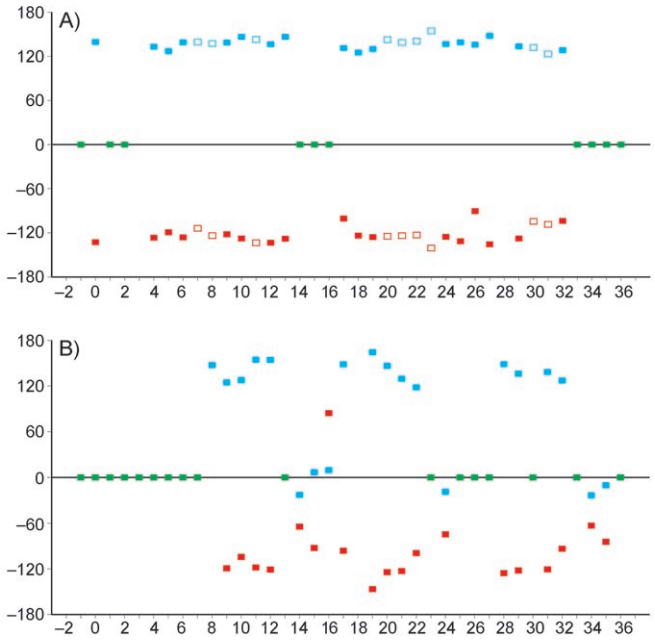

Figure 4. TALOS analysis for each residue: ψ dihedral angle (blue), ϕ dihedral angle (red), inconsistent predictions (green). A) CA150.WW2, fibril, B) CA150.WW2, native fold. Open symbols indicate predictions from ambiguous chemical shifts.

should be generally applicable to solid protein preparations that give intermediate line width or low amounts of sample—provided that the amino acid sequence is not highly repetitive and the protein is relatively small (<70 residues).

TALOS analysis revealed that the repeating unit of CA150.WW2 amyloid fibrils contains two long β strands separated by a short loop, a situation that is clearly different from the native WW fold. The C- and N-terminal residues not involved in the structural core of the amyloid fibril exhibited increased mobility, as detected in direct excitation ^{13}C spectra recorded by using a triply labelled fibril preparation. This sample was especially valuable due to improved line width observed in MAS NMR spectra; this indicates that deuteration might help to reduce the line width for other aggregation-prone protein sequences that have proved refractory to characterisation.

Experimental Section

Sample preparation: All MAS NMR spectroscopy samples of the Y19F variant of CA150.WW2 (with an N-terminal G−2S−1M0 sequence that arises from the vector) were expressed in *E. coli*, purified and fibrillised as described previously.[24,25] Five differently labelled samples were prepared: u-CA150.WW2 was uniformly ^{13}C,^{15}N-labelled; uniform ^{15}N labelling and ^{13}C labelling based on 2-^{13}C-glycerol and 1,3-^{13}C-glycerol was used in 2-CA150.WW2 and 1,3-CA150.WW2, respectively; d-CA150.WW2 was uniformly ^{2}H,^{13}C,^{15}N labelled and purified in water, which resulted in ^{1}H labelling at all exchangeable protons. A fifth sample was made by using specific labelling with u-^{13}C,^{15}N-glycine, u-^{13}C,^{15}N-alanine, 2,3-^{13}C,^{15}N-phenylalanine and 2,3-^{13}C,^{15}N-tyrosine. Approximately 15 mg of each preparation was centrifuged and transferred to a 4 or 3.2 mm ZrO_2 MAS rotor.

MAS NMR spectroscopy: ^{13}C–^{13}C correlations were recorded at a nominal temperature of 285 K by using either a Bruker AV900 or AV700; both were equipped with 3.2 and 4 mm MAS triple resonance probes. The ^{13}C–^{13}C-correlations were recorded for all samples by using a spinning frequency of 10.5 kHz (900 MHz) or 10.0 kHz (700 MHz). Carbon magnetization was produced by ramped cross polarization,[37] and transferred by using PDSD or dipolar-assisted rotational resonance (DARR) mixing during 20–700 ms.[38,39] Decoupling during direct and indirect evolution was performed at 80–85 kHz by using SPINAL-64 (small phase incremental alternation with 64 steps) or TPPM (two pulse phase-modulation).[40,41] For the d-CA150.WW2 sample spinning at 20 kHz and at a field of 900 MHz ^{13}C magnetization was excited directly and magnetization transfer was achieved by radio frequency driven recoupling (RFDR) by using mixing times between 1.2 and 4.8 ms.[42] WALTZ-16 decoupling at 5 kHz was applied during direct and indirect evolution.[43]

A newly designed 3D HNC-TEDOR experiment was recorded by using a Bruker AV600 machine, equipped with a 3.2 mm triple resonance probe, at a spinning frequency of 20 kHz. The pulse program and the phase cycling are depicted in Figure 5. The sequence started with a proton pulse and subsequent proton evolution and relied on fast MAS for proton decoupling in the deuterated sample. Then ^{15}N magnetisation was created by a short ramped CP, and after ^{15}N evolution a TEDOR period with 85 kHz SPINAL-64 proton decoupling followed. The experimental design was a modified version of earlier TEDOR experiments,[33,34] in which ^{15}N magnetisation was transferred to the ^{13}C nuclei by a REDOR pulse train followed by a pair of π/2 pulses. Detectable magnetisation was subsequently created by using a second REDOR pulse train. A total TEDOR mixing time of 1.2 ms was applied to favour one-bond correlations. Chemical shift referencing was done externally by using the downfield signal at 31.5 ppm in adamantane.[44]

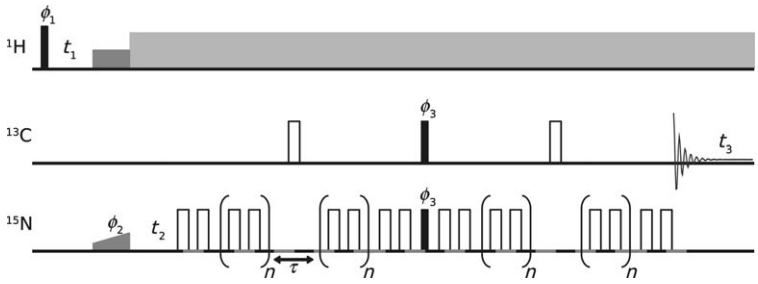

Figure 5. The 3D HNC-TEDOR pulse sequence, solid rectangles: π/2 pulses; open rectangles: π pulses; grey shapes: pulses of the CP transfer and proton decoupling (SPINAL-64); τ: length of one rotor period: n: pulses were repeated several times. Phase cycling was as follows: $\phi1 = y\ -y$, $\phi2 = -x\ -x\ -y\ -y\ x\ x\ y\ y$, $\phi3 = x\ x\ y\ y\ -x\ -x\ -y\ -y$, $\phi_{rec} = x\ -x\ y\ -y\ -x\ x\ -y\ y$; ^{15}N pulses were phase cycled according to the *xy* 16 scheme,[48] all other phases were *x*.

Solution NMR spectroscopy: u-CA150.WW2 (0.8 mM) was dissolved in sodium phosphate (pH 7.0, 20 mM, 0.02%, *w/v* Na_3N, 10% D_2O). The 2D ^{15}N-HSQC, 3D CBCA(CO)NH, 3D CBCANH, 3D (H)CC(CO)NH-TOCSY and 3D HNCO experiments were recorded at

285 K by using a Bruker DRX600 spectrometer equipped with a cryo probe.[45]

Data and chemical-shift analysis: Solid-state and solution NMR spectroscopy data were processed by using XWINNMR 2.6 (Bruker, Karlsruhe, Germany) or TOPSPIN 1.3 (Bruker, Karlsruhe, Germany). Data analysis and assignment were performed by using CCPN.[46] Figures were prepared by using Sparky 3.1 (T. D. Goddard, D. G. Kneller, University of California, San Francisco, USA). Chemical-shift analysis was done with TALOS.[47]

Acknowledgements

We thank Peter Schmieder for his help in setting up the solution NMR spectroscopy experiments. This work was funded by the Medical Research Council, UK, and the Deutsche Forschungsgemeinschaft, SFB449.

Keywords: amyloid fibrils · CA150 · deuteration · NMR spectroscopy · protein structures

[1] V. N. Uversky, A. L. Fink, *Biochim. Biophys. Acta Proteins Proteomics* **2004**, *1698*, 131–153.
[2] M. Stefani and C. M. Dobson, *J. Mol. Med.* **2003**, *81*, 678–699.
[3] O. S. Makin, L. C. Serpell, *FEBS J.* **2005**, *272*, 5950–5961.
[4] M. Sunde, L. C. Serpell, M. Bartlam, P. E. Fraser, M. B. Pepys, C. C. F. Blake, *J. Mol. Biol.* **1997**, *273*, 729–739.
[5] B. Caughey, P. T. Lansbury, *Annu. Rev. Neurosci.* **2003**, *26*, 267–298.
[6] M. Bucciantini, E. Giannoni, F. Chiti, F. Baroni, L. Formigli, J. S. Zurdo, N. Taddei, G. Ramponi, C. M. Dobson, M. Stefani, *Nature* **2002**, *416*, 507–511.
[7] A. S. Cohen, E. Calkins, *Nature* **1959**, *183*, 1202–1203.
[8] H. Puchtler, F. Sweat, *J. Histochem. Cytochem.* **1965**, *13*, 693–694.
[9] H. LeVine 3rd, *Protein Sci.* **1993**, *2*, 404–410.
[10] R. Nelson, M. R. Sawaya, M. Balbirnie, A. O. Madsen, C. Riekel, R. Grothe, D. Eisenberg, *Nature* **2005**, *435*, 773–778.
[11] M. R. Sawaya, S. Sambashivan, R. Nelson, M. I. Ivanova, S. A. Sievers, M. I. Apostol, M. J. Thompson, M. Balbirnie, J. J. W. Wiltzius, H. T. McFarlane, A. O. Madsen, C. Riekel, D. Eisenberg, *Nature* **2007**, *447*, 453–457.
[12] A. T. Petkova, Y. Ishii, J. J. Balbach, O. N. Antzutkin, R. D. Leapman, F. Delaglio, R. Tycko, *Proc. Natl. Acad. Sci. USA* **2002**, *99*, 16742–16747.
[13] T. Lührs, C. Ritter, M. Adrian, D. Riek-Loher, B. Bhormann, H. Döbeli, D. Schubert, R. Riek, *Proc. Natl. Acad. Sci. USA* **2005**, *102*, 17342–17347.
[14] K. Iwata, T. Fujiwara, Y. Matsuki, S. Takahashi, H. Naiki, Y. Goto, *Proc. Natl. Acad. Sci. USA* **2006**, *103*, 18119–18124.
[15] C. Ritter, M.-L. Maddelein, A. B. Siemer, T. Lührs, M. Ernst, B. H. Meier, S. J. Saupe, R. Riek, *Nature* **2005**, *435*, 844–848.
[16] A. B. Siemer, C. Ritter, M. O. Steinmetz, M. Ernst, R. Riek, B. H. Meier, *J. Biomol. NMR* **2006**, *34*, 75–87.
[17] A. Olofsson, J. H. Ippel, S. S. Wijmenga, E. Lundgren, A Öhman, *J. Biol. Chem.* **2004**, *279*, 5699–5707.
[18] H. Heise, W. Hoyer, S. Becker, O. C. Andronesi, D. Riedel, M. Baldus, *Proc. Natl. Acad. Sci. USA* **2005**, *102*, 15871–15876.
[19] K. D. Kloepper, D. H. Zhou, Y. Li, K. A. Winter, J. M. George, C. M. Rienstra, *J. Biomol. NMR* **2007**, *39*, 197–211.
[20] S. Luca, W.-M. Yau, R. Leapman, R. Tycko, *Biochemistry* **2007**, *46*, 13505–13522.
[21] A. T. Petkova, W.-M. Yau, R. Tycko, *Biochemistry* **2006**, *45*, 498–512.
[22] D. C. Chan, M. T. Bedford, P. Leder, *EMBO J.* **1996**, *15*, 1045–1054.
[23] N. Ferguson, C. M. Johnson, M. Macias, H. Oschkinat, A. Fersht, *Proc. Natl. Acad. Sci. USA* **2001**, *98*, 13002–13007.
[24] N. Ferguson, J. Berriman, M. Petrovich, T. D. Sharpe, J. T. Finch, A. Fersht, *Proc. Natl. Acad. Sci. USA* **2003**, *100*, 9814–9819.
[25] N. Ferguson, J. Becker, H. Tidow, S. Tremmel, T. D. Sharpe, G. Krause, J. Flinders, M. Petrovich, J. Berriman, H. Oschkinat, A. Fersht, *Proc. Natl. Acad. Sci. USA* **2006**, *103*, 16248–16253.
[26] J. Pauli, M. Baldus, B. van Rossum, H. de Groot, H. Oschkinat, *ChemBioChem* **2001**, *2*, 272–281.
[27] T. I. Igumenova, A. J. Wand, A. E. McDermott, *J. Am. Chem. Soc.* **2004**, *126*, 5323–5331.
[28] A. Lange, K. Giller, S. Hornig, M.-F. Martin-Eauclaire, O. Pongs, S. Becker, M. Baldus, *Nature* **2006**, *440*, 959–962.
[29] M. Etzkorn, S. Martell, O. C. A. Andronesi, K. Seidel, M. Engelhard, M. Baldus, *Angew. Chem.* **2007**, *119*, 463–466; *Angew. Chem. Int. Ed.* **2007**, *46*, 459–462.
[30] C. R. Morcombe, V. Gaponenko, R. A. Byrd, K. W. Zilm, *J. Am. Chem. Soc.* **2005**, *127*, 397–404.
[31] F. Castellani, B. van Rossum, A. Diehl, M. Schubert, K. Rehbein, H. Oschkinat, *Nature* **2002**, *420*, 98–102.
[32] P. E. Hansen, *Magn. Reson. Chem.* **2000**, *38*, 1–10.
[33] C. A. Michal, L. W. Jelinski, *J. Am. Chem. Soc.* **1997**, *119*, 9059–9060.
[34] C. P. Jaroniec, B. A. Tounge, C. M. Rienstra, J. Herzfeld, R. G. Griffin, *J. Magn. Reson.* **2000**, *146*, 132–139.
[35] M. J. Macias, V. Gervais, C. Civera, H. Oschkinat, *Nat. Struct. Biol.* **2000**, *7*, 375–379.
[36] T. Peng, J. S. Zintsmaster, A. T. Namanja, J. W. Peng, *Nat. Struct. Mol. Biol.* **2007**, *14*, 325–331.
[37] G. Metz, X. Wu, S. O. Smith, *J. Magn. Reson. Ser. A* **1994**, *110*, 219–227.
[38] N. M. Szeverenyi, M. J. Sullivan, G. E. Maciel, *J. Magn. Reson.* **1982**, *47*, 462–475.
[39] K. Takegoshi, S. Nakamura, T. Terao, *Chem. Phys. Lett.* **2001**, *344*, 631–637.
[40] B. M. Fung, A. K. Khitrin, K. Ermolaev, *J. Magn. Reson.* **2000**, *142*, 97–101.
[41] A. E. Bennett, C. M. Rienstra, M. Auger, K. V. Laksmi, R. G. Griffin, *J. Chem. Phys.* **1995**, *103*, 6951–6958.
[42] A. E. Bennett, J. H. Ok, R. G. Griffin, S. Vega, *J. Chem. Phys.* **1992**, *96*, 8624–8627.
[43] A. J. Shaka, J. Keeler, R. Freeman, *J. Magn. Reson.* **1983**, *53*, 313–340.
[44] C. R. Morcombe, K. W. Zilm, *J. Magn. Reson.* **2003**, *162*, 479–486.
[45] M. Sattler, J. Schleucher, C. Griesinger, *Prog. Nucl. Magn. Reson. Spectrosc.* **1999**, *34*, 93–158.
[46] W. F. Vranken, W. Boucher, T. J. Stevens, R. H. Foggh, A. Pajon, M. Llinas, E. L. Ulrich, J. L. Markley, J. Ionides, E. D. Laue, *Proteins Struct. Funct. Bioinf.* **2005**, *59*, 687–696.
[47] G. Cornilescu, F. Delagio, A. Bax, *J. Biomol. NMR* **1999**, *13*, 289–302.
[48] T. Gullion, D. B. Baker, M. S. Conradi, *J. Magn. Reson.* **1990**, *89*, 479–484.

Received: November 19, 2007
Published online on July 18, 2008

